EEG power spectra and subcortical pathology in chronic disorders of consciousness

Evan S. Lutkenhoff, Ph.D.[a,b], Anna Nigri, Ph.D [c], Davide Rossi Sebastiano, MD, Ph.D [d], Davide Sattin, PsyD [e], Elisa Visani, M.Sc. [d], Cristina Rosazza, Ph.D. [f], Ludovico D'Incerti, MD [c], Maria Grazia Bruzzone, MD [c], Silvana Franceschetti, MD [d], Matilde Leonardi, MD [e], Stefania Ferraro, Ph.D.[c,*], Martin M. Monti Ph.D.[a,b]

[a]*Department of Psychology, University of California Los Angeles, Los Angeles, CA, USA*
[b]*Brain Injury Research Center (BIRC), Department of Neurosurgery, David Geffen School of Medicine at UCLA, Los Angeles, CA, USA*
[c]*Department of Neuroradiology, Fondazione IRCCS Istituto Neurologico 'Carlo Besta', Milan, Italy.*
[d]*Department of Neurophysiology, Fondazione IRCCS Istituto Neurologico 'Carlo Besta', Milan, Italy.*
[e]*Neurology, Public Health, Disability Unit and Coma Research Centre, Fondazione IRCCS Istituto Neurologico 'Carlo Besta', Milan, Italy.*
[f]*Scientific Direction, Fondazione IRCCS Istituto Neurologico 'Carlo Besta', Milan, Italy.*
On the behalf of the Coma Research Center, Fondazione IRCCS Istituto Neurologico 'Carlo Besta', Milan, Italy.

*To whom correspondence should be addressed:

Stefania Ferraro, Ph.D.,

Fondazione IRCCS Neurologico 'Carlo Besta', Via Celoria 11, 20133 Milan, Italy,

Email: stefania.ferraro@istituto-besta.it,

Phone +39 (02) 23942397.

Abstract

Objective: To determine (i) the association between long-term impairment of consciousness after severe brain injury, spontaneous brain oscillations, and underlying subcortical damage, and (ii) whether such data can be used to aid patient diagnosis, a process known to be susceptible to high rates of error.

Methods: Cross-sectional observational sample of 116 patients with an acquired disorder of consciousness secondary to brain injury, collected prospectively at a tertiary center between 2011 and 2013. Multimodal analyses relating clinical measures of impairment, electroencephalographic measures of spontaneous brain activity, and magnetic resonance imaging data of subcortical atrophy were conducted in 2018.

Results: Systematic associations were found between electroencephalographic power spectra and subcortical damage. Specifically, the ratio of beta-to-delta relative power was negatively associated with greater atrophy in regions of the bilateral thalamus and globus pallidus (both left > right) previously shown to be preferentially atrophied in chronic disorders of consciousness. Power spectrum total density was also negatively associated with widespread atrophy in regions of the left globus pallidus, right caudate, and in brainstem. Furthermore, we showed that the combination of behavioral, encephalographic, and imaging data in an analytic framework can be employed to aid behavioral diagnosis.

Interpretation: These results associate, for the first time, electroencephalographic presentation, as detected with routine clinical techniques – thus grounding them in the

underlying brain pathology of disorders of consciousness – and demonstrate how multimodal combination of clinical, electroencephalographic, and imaging data can be employed in potentially mitigating the high rates of misdiagnosis typical of patients in this cohort.

Keywords: Consciousness, Electroencephalography, Magnetic Resonance Imaging, Severe Brain Injury

Introduction

Electroencephalography (EEG) and magnetic resonance imaging (MRI) are increasingly employed to monitor patient neurological status [1, 2], residual cognitive function [3-5], state of awareness [6-9], and potential for recovery [10-13] in patients with a disorder of consciousness (DOC; i.e., Coma, Vegetative State, VS; Minimally Conscious State 'minus,' MCS-; Minimally Conscious State 'plus,' MCS+; [14, 15]). In the context of bedside EEG, analysis of the magnitude of oscillations at different frequencies (i.e., power spectrum analysis), has shown capable of differentiating DOC patients from patients with severe neurocognitive disorder but no disorder of consciousness [16], as well as clinical categories of chronic DOC (i.e., VS, MCS), with depth of impairment being correlated with slower, and larger amplitude, oscillations [17, 18]. While this technique has been shown to be sensitive to different injury etiologies [19], it is blind to the underlying anatomical damage. At a theoretical level, the mesocircuit theory of recovery of consciousness after brain injury predicts a relationship between the slowing and amplitude of electrocortical oscillations and the degree of pathologic changes taking place after trauma, hypoxia, or multifocal ischemia [20]. In particular, under this view, the evolving damage occurring after severe brain injury results in a reduction of thalamo-cortical and thalamo-striatal excitatory outflow, due to deafferentation and loss of neurons in central thalamus, which leads to a net decrease in excitatory input to the forebrain and striatum [20]. While indirect evidence exists in support of this model, with *in vivo* and *post-mortem* works demonstrating a relationship between damage to thalamus, loss of thalamo-cortical structural

connectivity, and depth of impairment [21-23], there is virtually no data directly uniting the patterns of EEG power spectra at the scalp in bedside recordings and patterns of subcortical damage in long-term DOC patients, a gap which is not only problematic for the clinician's interpretation of the observed EEG data, but also hampers our ability to monitor, through an unexpensive, repeatable technique, easily applicable at the patient's bedside, interventions and their effects. In what follows, we address, in a large cohort of patients with chronic DOC, the heretofore untested relationship between observed electrocortical rhythms, patterns of subcortical brain atrophy (including thalamus, brainstem, and basal ganglia), and behavioral measures of awareness and arousal, as indexed by the Coma Recovery Scale-revised (CRS-R; [24]).

Methods

Participants

A consecutive sample of 116 patients was recruited from a larger database (n = 153) of adult chronic DOC patients with acquired acute severe brain injury, who underwent a 1-week program of clinical multimodal assessments during 2011-2013 at the Coma Research Centre (CRC) of the Neurological Institute C. Besta in Milan, Italy. The assessment included (i) clinical evaluation with the CRS-R [24], (ii) a multiple neurophysiological evaluation including a long-lasting EEG, and (iii) neuroradiological assessment including a structural T1-weighted MRI. The patient cohort was also described in previous works of our group [25-28].

	VS	MCS-	MCS+
Age (mean, SD, y)	53 (±14.21)	54 (±18.77)	46 (±16.77)
MPI (mean, SD, mo)	23 (±16.05)	44 (±37.17)	53 (±64.97)
Sex	14F, 23M	11F, 6M	0F, 7M
Etiology	12T, 9H, 1I, 1HI, 14TA	5T, 7H, 1I, 0HI, 4TA	3T, 3H, 1I, 0HI, 0TA
Coma Recovery Scale Revised (CRS-R)			
Total score	6.24 (1.01)	9.24 (1.25)	10.43 (1.90)
Auditory	1.03 (0.50)	1.41 (0.51)	2.00 (1.15)
Visual	0.76 (0.43)	2.59 (0.71)	2.43 (1.40)
Motor	1.92 (0.28)	2.12 (0.33)	2.14 (0.90)
Orom/Verb	1.00 (0.33)	1.24 (0.56)	1.43 (0.98)
Communic	0.00 (0.00)	0.12 (0.33)	0.57 (0.53)
Arousal	1.54 (0.56)	1.76 (0.56)	1.86 (0.90)
Electroencephalography (Total power & frequency relative power)			
Total power (μV^2)	138.22 (140.35)	229.20 (261.81)	178.96 (148.15)
Delta (1–4Hz)	49.46% (13.46%)	41.51% (14.35%)	42.57% (16.97%)
Theta (4–8Hz)	30.21% (11.09%)	34.09% (9.73%)	33.23% (11.58%)
Alpha (8–13Hz)	9.71% (5.64%)	11.89% (6.08%)	8.33% (4.48%)
Beta (13–30Hz)	7.78% (7.09%)	9.59% (8.22%)	13.89% (17.23%)
Gamma (>30Hz)	2.84% (3.00%)	2.91% (3.21%)	1.98% (1.63%)

Table 1: Analyzed sample summary statistics of demographic, clinical, and electroencephalographic data per diagnostic group. (Abbreviations: VS, Vegetative State; MCS- Minimally conscious State "minus"; MCS+, Minimally Conscious State "plus"; MPI, months post-injury; T, traumatic; NT, non-traumatic; H, hemorrhagic injury, I, ischemic injury, A, anoxic; Orom/Verb, oromotor/verbal; Communic, communication.)

The acquisition of both EEG and structural MRI (T1-weighted) datasets, constituted the inclusion criteria for each patient. Experienced raters independently assessed each patient 4 times with the Italian version of the CRS-R [29]; the best recorded performance was used to classify the patient as VS or MCS. As described below, 55 patients were discarded due to the low quality of the MRI data (e.g. motion during the data acquisitions) in agreement with the procedure described previously [21]. The final sample was constituted by 61 patients with DOC (median age= 53 years, range age = 20-82 years, 36 males): 37 patients were classified as VS and 24 as MCS. In regard to the etiology of DOC, 33% of the patients (n = 20) suffered from traumatic brain injury (TBI), while 67% (n = 41) from non-traumatic brain injury (non-TBI). In particular, among non-TBI patients, 30% (n = 18) suffered from anoxic brain injury and 37% (n = 23) from haemorrhagic brain injury and/or ischemic brain injury. The median disease duration at the time of the study was 24 months (range = 5-198 months). (See Table S1). The local Ethics Committee approved all aspects of this research and written informed consent was obtained from the legally authorized representative of the patients prior to their inclusion in the study.

Data acquisition and analysis

EEG data acquisition and processing

As described previously [28], patients underwent polygraphic recordings between 2 p.m. and 9 a.m. on the following day. Recordings included electrooculography (EOG), electromyography (EMG) from the sub-mental muscle, a bipolar precordial electrocardiogram (ECG) derivation and an impedance thoracic pneumogram. EEG recordings were made with Ag/AgCl surface electrodes (impedance was kept < 5*k*Ω)

and acquired at a sampling rate of 256 Hz using a computerized system (Micromed SpA, Mogliano Veneto, Treviso, Italy). The raw EEG signals were recorded against a common reference electrode in order to allow off-line data reformatting, using a 19 EEG electrode array placed according to the 10-20 International System (including frontal (Fp1, Fp2, F3, F4), central (C3, C4), parietal (P3, P4), and occipital (O1, O2) electrodes). The spectral EEG analysis was performed on 5-minutes, consecutive, artifact-free awake EEG epochs starting from 10 s after the end of the response to an arousal stimuli, when the EMG artifacts had virtually disappeared and the patients had closed their eyes, but in the absence of any change in the EEG or polygraphic parameters suggesting sleep. The EEG epochs with continuous epileptiform activities (e.g. periodic lateralized epileptiform discharges) were discarded. The selected EEG epochs were filtered (1-70 Hz, 12 db/octave) followed by a 50 Hz notch filter to suppress the noise of the electrical power line, were reformatted against the linked ear-lobe reference, and analyzed using the fast Fourier transform. Then, the selected EEG activity was analyzed by dividing it into 90 non-overlapping 2 s segments. Absolute total power and relative power were evaluated in the delta (1-4 Hz), theta (4-8 Hz), alpha (8-13 Hz), beta (13-30 Hz) and gamma (>30 Hz) bands, and averaged within each EEG channel.

MRI data acquisition and processing

Neuroimaging data were obtained with a 3T MR scanner (Achieva, Philips Healthcare BV, Best, NL) equipped with a 32-channel head coil. The MRI protocol comprised a high resolution 3D-TFE T1-weighted sequence (185 sagittal slices, TR = 9.781 ms, TE

= 4.6 ms, FOV = 240 × 240 mm^2, voxel size = 1 × 1 × 1 mm^3, flip angle = 8°). Analysis of subcortical structures was conducted using a technique known as shape or vertex analysis, part of the FMRIB software library (FSL; FMRIB, Oxford, UK), following a previously established pipeline [13, 21]. Briefly, MR images were brain-extracted using optiBET [30], then the thalamus, caudate, putamen, globus pallidus, hippocampus, and brainstem were segmented using FSL FIRST [31], for each patient and structure separately, and then reconstructed into 3-dimensional vertex meshes, as depicted in Figure 1. In addition, the intracranial volume (ICV), a measure of global atrophy including white and gray matter volume, was calculated for each patient using a modified FSL SIENA algorithm [32].

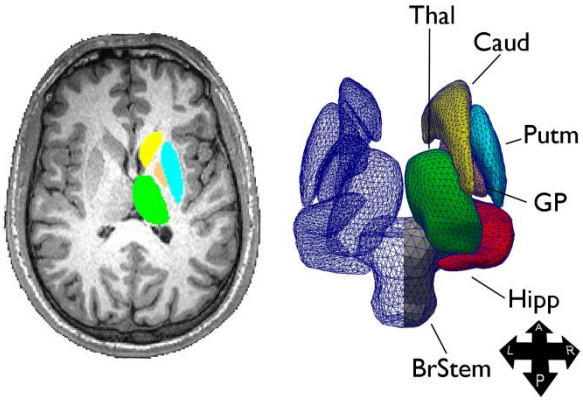

Figure 1: Sample structure extraction (left) and 3-dimensional triangle vertex mesh (right). (Abbreviations: A, anterior; BrStem, brain stem; Caud, caudate; GP, globus pallidus; Hipp, hippocampus; L, left; P, posterior; Putm, putamen; R, right; Thal, thalamus. Figure from[21].)

Statistical Analyses

In what follows, we describe the four analyses we performed. First, we assessed the EEG spectral data and their association with depth of the DOC. Following, we assessed

how the MRI measures of subcortical atrophy are related to the EEG power spectral data and to the behavioral presentation (i.e., CRS-R). Finally, we brought together demographic, MRI and EEG data into an analytic model (i.e., binary logistic regression) attempting to separate VS from MCS patients.

EEG analysis

To assess the relationship between EEG spectral power and its relation to clinical grouping, we ran a mixed-model linear analysis with EEG (relative) power as the dependent variable, laterality (left, right, middle), channel position (Fp, F, C, P, O), and EEG features (total power, delta, theta, alpha, beta, gamma bands) as the repeated measures, diagnosis (VS, MCS-, MCS+), etiology (TBI, non-TBI), sex, frequency, age, and months post-injury as fixed variables and subjects as the random variable. As described below, the significant interaction between EEG features and diagnosis was followed up with one mixed-model analysis per each EEG feature (using the same model, albeit without the EEG feature as repeated variable). Individual mixed-models were followed up with pairwise post-hoc comparisons between diagnostic groups (i.e., VS, MCS-, MCS+), with Sidak correction for multiple comparisons.

EEG – MRI analysis

We related relative EEG spectral features to subcortical local shape change measures. Prior to performing this analysis, however, because of significant correlations among spectral characteristics across electrodes and frequency bands, spectral data were entered into a principal component analysis (PCA; performed in SAS), with varimax rotation . The PCA performed on EEG power data returned 8 components with

eigenvalue greater than 1, cumulatively explaining 91.8% of the total variance. The first three components presented a similar pattern, each loading negatively on all the delta band electrodes and positively on beta, alpha, and theta electrodes bands respectively (henceforth, β/δ ratio component, α/δ ratio component, and θ/δ ratio component, respectively). The fourth component loaded positively on all gamma frequency electrodes (henceforth, gamma component), while the fifth component loaded positively on the total power for each electrode (henceforth, total power component). Finally, the last three components appeared to capture diffuse statistical covariance between electrodes, although with a preference for loading positively upon the right hemispheric delta band channels and negatively on the right hemispheric alpha band channels (henceforth, δ/α_{RH} ratio component), loading positively on delta band in Fp channels and negatively on the alpha band channels in those same electrodes (henceforth, δ/α_{Fp} ratio component), and loading negatively on both the alpha and theta band in the parietal and occipital electrodes (henceforth, $\alpha\theta_{(\mathrm{P,O})}$*[Neg.]*). EEG components were then entered, as independent variables, in a general linear model attempting to capture associations with localized shape patterns (e.g., atrophy). The analysis also included, as covariates, sex, age, time-post-injury, etiology (i.e., TBI vs non-TBI), and ICV (to ensure that observed tissue displacement reflect local subcortical shape changes independent of overall brain atrophy). Group-level significance was assessed with a non-parametric permutation test at a level of $p < 0.05$ corrected for multiple comparisons using a family-wise cluster correction and threshold free cluster enhancement (TFCE) as implemented in FSL randomize [33, 34].

CRS-R – MRI analysis

In this analysis, we related the patients' behavioral presentation, as captured by the CRS-R subscales, with subcortical atrophy. Because of significant correlations between the subscales of the CRS-R (i.e., the desired independent variables), behavioral data were entered into a PCA performed analogously to the one described above. The analysis returned 3 components with an eigenvalue greater than 1, cumulatively explaining 69.57% of the variance. The three components were loaded upon by, respectively, the auditory, visual, and arousal subscales (henceforth, audio-video-arousal component), the motor subscale (henceforth, motor component), and the oromotor and communication subscales (henceforth, oromotor-communication component). As in the previous analysis, the three components were entered in a general linear model, as independent variables, attempting to capture systematic associations with shape patterns, along with the same covariates described above. Group-level significance was assessed similarly to the previous analysis.

Predicting DOC level from EEG spectral features

Finally, we employed a binary logistic regression to evaluate the degree to which global atrophy and EEG measures related to diagnosis (i.e., VS vs. MCS). With a 3-block model, we attempt to predict diagnosis from a model including demographic variables only (i.e., age, sex, months post injury, etiology (TBI vs. non-TBI)), a model including demographic and a measure of global atrophy (including global white matter and gray matter), and a model including demographics, global atrophy, and EEG variables (i.e., the 8 EEG components).

Results

EEG results

The mixed-model analysis revealed a significant interaction ($F(10, 1309.055) = 16.599$, $p < 0.001$) between diagnostic group (i.e., VS, MCS-, MCS+) and EEG features (i.e., total power, delta, theta, alpha, beta, gamma frequency bands; see Figure 2 and Table 3), along with a significant main effect of diagnosis ($F(2, 4389.124) = 5.158$, $p = 0.006$), EEG features $F(5, 1309.055) = 6.368$, $p < 0.001$), and months post-injury ($F(2, 4220.566) = 5.407$, $p = 0.020$). Follow-up mixed-model analyses (one per EEG feature) revealed a significant effect of diagnosis on total power ($F(2, 594.374) = 19.115$, $p < 0.001$; with pairwise-comparisons revealing that VS patients show significantly less total power than both MCS groups), delta ($F(2, 770.006) = 4.620$, $p = 0.010$; with VS patients having the most relative delta power, significantly more than MCS- patients), theta ($F(2, 779.789) = 12.268$, $p < 0.001$; with VS showing significantly less relative theta power than both MCS groups, and MCS- showing marginally ($p = 0.077$) less relative theta power than MCS+), alpha ($F(2, 748.766) = 13.231$, $p < 0.001$; with MCS- patients showing significantly more relative alpha power than VS and MCS+, and VS showing greater relative alpha power than MCS+), and gamma ($F(2, 746.625) = 5.416$, $p = 0.005$; with MCS+ patients showing significantly less relative gamma power than MCS- and marginally ($p = 0.058$) less than VS patients). (For further description of the EEG data in this cohort see [28].)

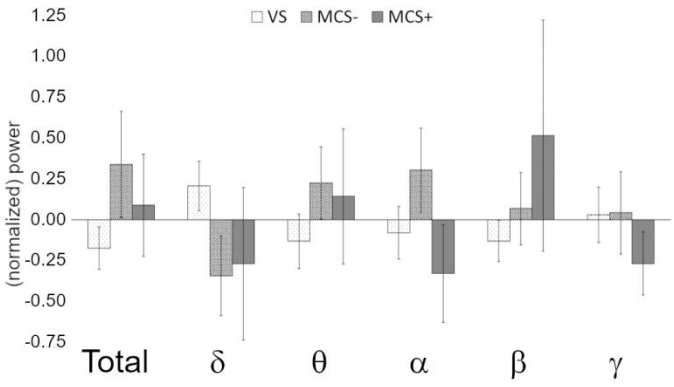

Figure 2: Summary of EEG data. Total and relative power at each frequency band (to allow displaying on the same axis, values are normalized within each variable). (Error bars represent standard errors.)

EEG – MRI analysis

As shown in Figure 3, three of the EEG factors exhibited significant correlations with local atrophy measurements. Specifically, the β/δ ratio component was negatively associated with greater atrophy in bilateral thalamus (left: t = 3.28, p = 0.025, 1,007 significant vertices [sig. vert.], right: t = 2.85, p = 0.041, 544 sig. vert.), bilateral globus pallidus (left: t = 4.26, p = 0.002, 491 sig. vert.; right: t = 3.42, p = 0.025, 356 sig. vert.), left caudate (t = 3.37, p = 0.02, 793 sign. vert.), and right hippocampus (t = 3.21, p = 0.02, 735 sig. vert.) (see Fig. 3a). The θ/δ component was negatively associated with increased atrophy in right putamen (t = 3.72, p = 0.037, 140 sig. vert.) and right globus pallidus (t = 3.89, p = 0.037, 30 sig. vert.) (see Fig. 3b). Finally, the total power component was negatively associated with widespread atrophy in the brainstem (including the 4th ventricle region; t = 4.41, p = 0.004, 3704 sig. vert.), as

well as the left globus pallidus (t = 4.00, p = 0.008, 365 sig. vert.) and right caudate (t = 5.48, p = 0.018, 193 sig. vert.) (see Fig. 3c). No significant associations were detected for any of the remaining components.

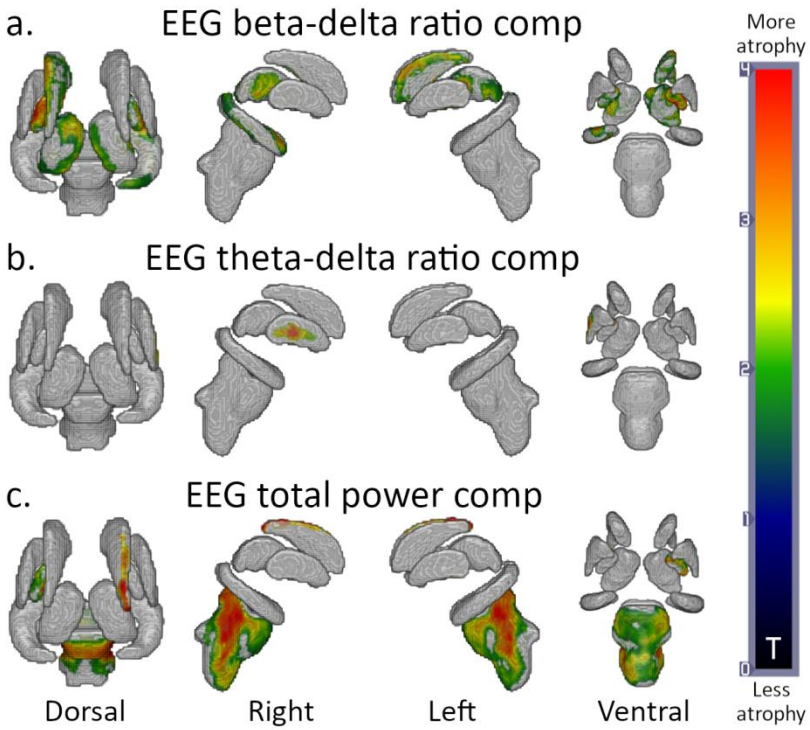

Figure 3: Results for the rest EEG – MRI analysis. (a) Results for the β/δ ratio component; (b) results for the θ/δ component; (c) results for the total power component. Hot colors indicate regions with significant greater atrophy; gray indicates no significant effect.

CRS-R – MRI analysis

As shown in Figure 4a,b, two of the CRS-R components exhibited significant correlations with local atrophy measurements. Specifically, the motor component was negatively associated with greater atrophy in broad regions of the brainstem (t = 3.69, p = 0.074, 4,301 sig. vert.; see Fig. 4a) while the oromotor-communication component was negatively associated with greater atrophy in regions of the brainstem (t = 2.74, p = 0.05, 943 sig. vert.), left putamen (t = 3.23, p = 0.023, 712 sig. vert.), and right globus pallidus (t = 2.38, p = 0.049, 108 sig. vert.). A large, but only marginally significant, clusters was also observed in left thalamus (t = 2.36, p = 0.06, 928 sig. vert.) (see Fig. 4b).

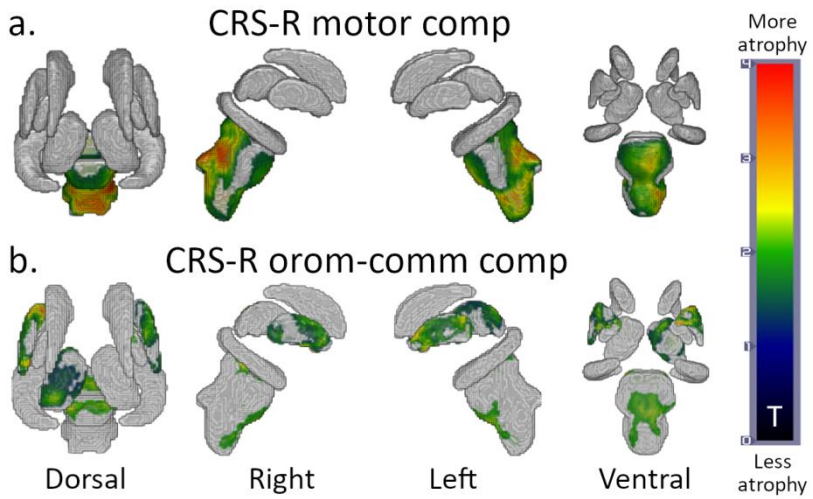

Figure 4: Results for the CRS-R – MRI analyses. (a) results for the CRS-R motor component; (b) results for the CRS-R oromotor-communication component. (See Fig. 3 for color interpretation.)

Predicting DOC level from EEG spectral features

As shown in Figure 5a and Table 2, diagnosis (i.e., VS vs. MCS) was predicted significantly better by the model including EEG components, overall brain atrophy (including both white matter and gray matter), and demographic components (i.e., age, sex, etiology (TBI vs. non-TBI), and months post injury; $\chi^2(54) = 29.09$, $p < 0.001$, Nagelkerke pseudo-$R^2_{Nag} = 0.51$), compared to the model with demographics and brain atrophy ($\chi^2(58)=16.66$, $p < 0.001$, $R^2_{Nag} = 0.32$), as well as the model with demographics only (χ^2 (59) = 8.93, $p = 0.003$, $R^2_{Nag} = 0.18$). Indeed, the full model achieved better performance as area under the curve ($AUC = 0.87$), sensitivity and specificity (sens/spec; 0.79, 0.81, respectively) than both other models ($AUC = 0.78$, sens/spec 0.58/0.78 and $AUC = 0.67$, sens/spec 0.29/0.89 for the behavioral and atrophy and the behavioral only models, respectively). Notably, the contribution of increasingly complex model (i.e., adding brain atrophy and EEG components) is to increase the model's sensitivity to MCS (at the cost of a decrease in specificity). Finally, in terms of individual variables, as shown in Figure 5b and Table 2, the full model selected one behavioral component (age/sex; $\beta = 1.44$, $OR = 1.06$, $p = 0.002$), overall brain atrophy ($\beta = 1.27$, $OR = 3.56$, $p < 0.001$), as well as the EEG total power ($\beta = 0.66$, $OR = 1.94$, $p = 0.017$), and, though only marginally significant, the EEG θ/δ ratio component ($\beta = 0.61$, $OR = 1.84$, $p = 0.06$).

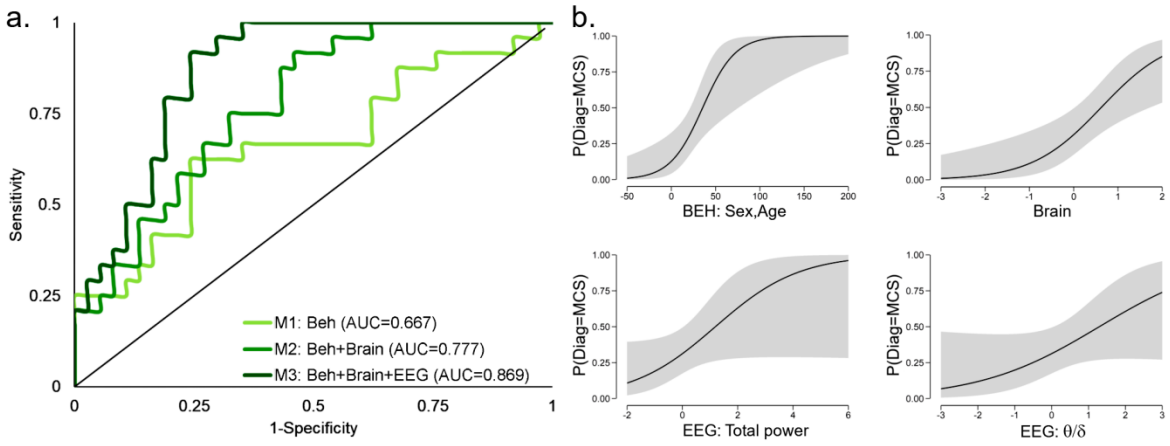

Figure 5: (a) ROC curve for the three binary logistic models classifying patient diagnosis (i.e., VS versus MCS) on the basis of behavioral components alone (M1), behavioral components and overall brain atrophy (M2), and behavioral components, brain volume, and EEG components (M3). (b) Conditional estimate plots for each of the significant variables selected in the full model; top row: Behavioral age and sex component, brain overall atrophy (i.e., ICV); bottom row: EEG total power component, EEG theta/delta component).

Model	df	ΔX^2	p	R^2	AUC	Sensitivity	Specificity	Precision
Intercept	60							
BEH	59	8.93	0.003	0.18	0.67	0.29	0.89	0.64
BEH+Brain	58	16.66	<0.001	0.32	0.78	0.58	0.78	0.64
BEH+Brain+EEG	54	29.09	<0.001	0.51	0.87	0.79	0.81	0.73

							95% CI	
Parameter	b	SE	β	OR	z	p	LB	UB
(Intercept)	-1.92	0.50	-0.79	0.15	-3.86	<0.001	-2.89	-0.95
BEH: Sex-Age	0.05	0.02	1.44	1.06	3.15	0.002	0.02	0.09
Normalized Brain	1.27	0.37	1.27	3.56	3.44	<0.001	0.55	1.99
EEG: Total power	0.66	0.28	0.66	1.94	2.39	0.017	0.12	1.21
EEG: $\delta/\alpha(RH)$	0.63	0.57	0.63	1.88	1.11	0.269	-0.49	1.75
EEG: θ/δ	0.61	0.32	0.61	1.84	1.88	0.060	-0.03	1.25
EEG: $\alpha\theta(P,O)[Neg.]$	0.59	0.36	0.59	1.80	1.65	0.100	-0.11	1.29

Table 2: Binary logistic regression results. Top: comparison of the AUC, sensitivity, specificity, and precision of the model with behavioral components only, the model with behavioral components and the brain normalization factor, and the model with behavioral components, brain normalization factor, and EEG components. Bottom: Individual predictors selected for the full model (i.e., BEH+Brain+EEG).

Discussion

In this work we report three main findings addressing the relationship between severity of the impairment of consciousness EEG spectral profile, and sub- cortical atrophy. First, our results show that spectral profiles recorded with conventional EEG map onto specific patterns of subcortical brain pathology (as observed with MRI), in line with a recent proposal. [20, 35] Indeed, we find that the ratio of fast (i.e., beta) to slow (i.e., delta) frequencies is related to atrophy in thalamic regions well known to be associated with severity of impairment after brain injury, as shown in *post-mortem* [36] and *in vivo* [21, 37, 38] studies, putatively secondary to delayed injury. Damage within thalamus, along with functional [4] and/or structural disconnection of thalamo-cortical projections [23], is indeed central to current theories of recovery from severe brain injury [35], and might be key to the network dysfunction and inferred loss of information processing measured with advanced neuroimaging approaches [6, 7, 26, 28, 39, 40]. Furthermore, a recent cross-modal study in the acute and sub-acute patients has shown that EEG spectral profiles dominated by slow frequencies (i.e., delta) are predictive of poor outcome and increased thalamic atrophy at 6 months post injury in moderate-to-severe TBI patients recovering from coma [13]. Indeed, interventions aimed at up-regulating thalamic activity have been shown to be capable of enhancing (to different degrees) behavioral responsiveness in patients suffering from severe brain injury [41-45].

Second, similarly to results obtained in a different (large) cohort of chronic DOC patients [21], subscales of the CRS-R mapped onto different underlying patterns of atrophy, with oromotor/verbal and communication subscales component loading on left

thalamic and bilateral putamen, as well as subregions of brainstem, and the motor component loading mainly on extensive brainstem atrophy. While the present results are generally similar to those reported previously [21], there also are important differences. For example, no brainstem atrophy was observed in the previous work, and the pattern of thalamic atrophy in the two studies is not fully overlapping. It is difficult, however, to fully evaluate the meaning of these differences since the PCA components extracted in the two studies loaded differently on each CRS-R subscale. So although we do find a consistent set of regions correlating with CRS-R communication subscale in the two studies, spanning left thalamus and putamen, the details of the associations between the full panel of subscales and subcortical brain pathology remain to be fully characterized. Finally, and most crucially from the clinical point of view, we have shown that EEG spectral features are relevant to diagnosing a patient's chronic state of consciousness (i.e., VS versus MCS), a decision known to be susceptible to a relatively high misdiagnosis rate [4, 46-48]. Specifically, EEG components, together with demographic information, could correctly classify patients across the conscious/unconscious line (as behaviorally defined) with ~87% success, leveraging on behavioral information (i.e., sex, age), overall brain atrophy, and EEG features (i.e., total power and θ/δ components). Despite the good concordance between behavior-based diagnosis and the classification based on demographic, brain atrophy, and EEG variables, the two approaches still disagree over one third of the cases. Specifically, seven MCS patients were classified as being in VS and seven VS patients were classified as being MCS. The MCS patients classified as VS by our analysis could

either reflect the fact that the patient was transiently unconscious at the time of EEG data acquisition, as characteristic of MCS patients [15], or the fact that behavioral diagnoses compress very different EEG profiles into the same clinical category. Similarly, the VS patients classified as MCS by our algorithm could either be a reflection of the variance in the spectrum of oscillations that are compatible with a state of unconsciousness, or a genuine misdiagnosis [4, 9, 49]. In evaluating the above results, the reader should be mindful of some limitations in our approach. First, as is often the case in the context of chronic DOC, our results are skewed by survivor bias effects; we might thus be representing a spectrum of impairment which, while severe, excludes the even greater damage present in patients who do not survive until over a year post injury. Second, due to significant correlations across channels within and across power bands, in order to perform the regression analyses presented above we had to first reduce the independent variables by means of a PCA. While this is conventional, it does affect the interpretation of our results in as much as we cannot directly assess whether the effects we report in mixed component (e.g., the β/δ component) are principally due to either frequency or to their combination. Third, gamma frequencies are known to often contain residual muscle artifacts; a reason why they are often excluded in analyses. Here we decided to keep them mainly because, even if they do contain artefacts, including the gamma component still contributes to explaining variance in the signal (even if we cannot tell if their variance is due to brain processes, motion, or a combination of the two). Had we not included it, any variance across patients due to motion would have *de facto* been subsumed by the unexplained

variance term thereby making our statistical estimates more conservative. In this sense, our approach is analogous, to give an example, to the conventional inclusion of motion parameters in functional MRI studies. Finally, we stress that while we report associations between brain damage in subcortical regions and EEG spectral features, this does not necessarily imply that the pinpointed areas are, themselves, the generators of specific oscillatory rhythms at rest.

In conclusion, the present work begins bridging very different levels of analysis of patients surviving severe brain injury, uniting brain pathology in subcortical regions considered to be key to DoC [35], clinical evaluation [24], and power spectral features [1, 13, 19]. Furthermore, our data show that such multimodal approaches are not only important from the point of view of basic research, but can also be employed in the context of diagnosis, something that is known to be particularly challenging in this patient cohort [46-48].

Importantly, our techniques – while novel in their current multimodal application – are entirely based on conventional clinical data (for both EEG and MRI) and on analysis pipelines that have been well validated in populations with severe brain pathology [30] and are freely available, implying that the methods we presented are relevant and directly translatable to clinical practice. Furthermore, the present data also show that the pattern of association between spectral profile, brain damage, and clinical variables observed in the acute setting [13] persist through the chronic time frame, in line with the idea that brain injury is best thought of as a long-term disease as opposed to an “event” [50].

Author Contributions

SF, MMM, ML, MGB conceived the study; DRS, SF, EV, oversaw collection and clinical interpretation of EEG data; LD, MGB, AN, CR oversaw collection and clinical interpretation of MRI data; ESL, AN, carried out the analysis presented in the paper; ESL, AN, SF, MMM, interpreted the results and drafted the manuscript; all authors provided critical feedback on the manuscript; SF, MMM, MGB secured funding.

Potential Conflicts of Interest

The Authors declare no conflicts of interest.

Funding sources

This work was supported by the Italian Ministry of Health (research grant RF-2013-02359287) and by Tiny Blue Dot Foundation.

References

1. Brenner RP. The interpretation of the EEG in stupor and coma. Neurologist 2005;11:271-284.

2. Young GB, McLachlan RS, Kreeft JH, Demelo JD. An electroencephalographic classification for coma. Can J Neurol Sci 1997;24:320-325.

3. Chennu S, Finoia P, Kamau E, et al. Dissociable endogenous and exogenous attention in disorders of consciousness. Neuroimage Clin 2013;3:450-461.

4. Monti MM, Rosenberg M, Finoia P, Kamau E, Pickard JD, Owen AM. Thalamo-frontal connectivity mediates top-down cognitive functions in disorders of consciousness. Neurology 2015;84:167-173.

5. Schnakers C, Perrin F, Schabus M, et al. Voluntary brain processing in disorders of consciousness. Neurology 2008;71:1614-1620.

6. Chennu S, Finoia P, Kamau E, et al. Spectral signatures of reorganised brain networks in disorders of consciousness. PLoS Comput Biol 2014;10:e1003887.

7. Crone JS, Schurz M, Holler Y, et al. Impaired consciousness is linked to changes in effective connectivity of the posterior cingulate cortex within the default mode network. Neuroimage 2015;110:101-109.

8. Demertzi A, Tagliazucchi E, Dehaene S, et al. Human consciousness is supported by dynamic complex patterns of brain signal coordination. Science 2019;5:eaat7603.

9. Owen AM, Coleman MR, Boly M, Davis MH, Laureys S, Pickard JD. Detecting awareness in the vegetative state. Science 2006;313:1402.

10. Bagnato S, Boccagni C, Prestandrea C, Sant'Angelo A, Castiglione A, Galardi G. Prognostic value of standard EEG in traumatic and non-traumatic disorders of consciousness following coma. Clin Neurophysiol 2010;121:274-280.

11. Crone JS, Bio BJ, Vespa PM, Lutkenhoff ES, Monti MM. Restoration of thalamo-cortical connectivity after brain injury: recovery of consciousness, complex behavior, or passage of time? J Neurosci Res 2018;96:671-687.

12. Schnakers C, Ledoux D, Majerus S, et al. Diagnostic and prognostic use of bispectral index in coma, vegetative state and related disorders. Brain Inj 2008;22:926-931.

13. Schnakers C, Lutkenhoff ES, Bio BJ, McArthur DL, Vespa PM, Monti MM. Acute EEG spectra characteristics predict thalamic atrophy after severe TBI. J Neurol Neurosurg Psychiatry 2018.

14. Bruno MA, Vanhaudenhuyse A, Thibaut A, Moonen G, Laureys S. From unresponsive wakefulness to minimally conscious PLUS and functional locked-in syndromes: recent advances in our understanding of disorders of consciousness. J Neurol 2011;258:1373-1384.

15. Monti MM, Laureys S, Owen AM. The vegetative state. BMJ 2010;341:c3765.

16. Leon-Carrion J, Martin-Rodriguez JF, Damas-Lopez J, Barroso y Martin JM, Dominguez-Morales MR. Brain function in the minimally conscious state: a quantitative neurophysiological study. Clin Neurophysiol 2008;119:1506-1514.

17. Lechinger J, Bothe K, Pichler G, et al. CRS-R score in disorders of consciousness is strongly related to spectral EEG at rest. Journal of Neurology 2013;260:2348-2356.

18. Lehembre R, Bruno MA, Vanhaudenhuyse A, et al. Resting-state EEG study of

comatose patients: a connectivity and frequency analysis to find differences between vegetative and minimally conscious states. Functional Neurology 2012;27:41-47.

19. Fingelkurts AA, Fingelkurts AA, Bagnato S, Boccagni C, Galardi G. The value of spontaneous EEG oscillations in distinguishing patients in vegetative and minimally conscious states. Suppl Clin Neurophysiol 2013;62:81-99.

20. Schiff ND. Mesocircuit mechanisms underlying recovery of consciousness following severe brain injuries: model and predictions. Brain Function and Responsiveness in Disorders of Consciousness: Springer, 2016: 195-204.

21. Lutkenhoff ES, Chiang J, Tshibanda L, et al. Thalamic and extrathalamic mechanisms of consciousness after severe brain injury. Ann Neurol 2015;78:68-76.

22. Maxwell WL, Pennington K, MacKinnon MA, et al. Differential responses in three thalamic nuclei in moderately disabled, severely disabled and vegetative patients after blunt head injury. Brain 2004;127:2470-2478.

23. Zheng ZS, Reggente N, Lutkenhoff E, Owen AM, Monti MM. Disentangling disorders of consciousness: Insights from diffusion tensor imaging and machine learning. Hum Brain Mapp 2017;38:431-443.

24. Giacino JT, Kalmar K, Whyte J. The JFK Coma Recovery Scale-Revised: measurement characteristics and diagnostic utility. Arch Phys Med Rehabil 2004;85:2020-2029.

25. Nigri A, Catricala E, Ferraro S, et al. The neural correlates of lexical processing in disorders of consciousness. Brain Imaging Behav 2017;11:1526-1537.

26. Rosazza C, Andronache A, Sattin D, et al. Multimodal study of default-mode

network integrity in disorders of consciousness. Ann Neurol 2016;79:841-853.

27. Rossi Sebastiano D, Panzica F, Visani E, et al. Significance of multiple neurophysiological measures in patients with chronic disorders of consciousness. Clin Neurophysiol 2015;126:558-564.

28. Rossi Sebastiano D, Visani E, Panzica F, et al. Sleep patterns associated with the severity of impairment in a large cohort of patients with chronic disorders of consciousness. Clin Neurophysiol 2018;129:687-693.

29. Sacco S, Altobelli E, Pistarini C, Cerone D, Cazzulani B, Carolei A. Validation of the Italian version of the Coma Recovery Scale-Revised (CRS-R). Brain Inj 2011;25:488-495.

30. Lutkenhoff ES, Rosenberg M, Chiang J, et al. Optimized brain extraction for pathological brains (optiBET). PLoS One 2014;9:e115551.

31. Patenaude B, Smith SM, Kennedy DN, Jenkinson M. A Bayesian model of shape and appearance for subcortical brain segmentation. Neuroimage 2011;56:907-922.

32. Smith SM, Zhang Y, Jenkinson M, et al. Accurate, robust, and automated longitudinal and cross-sectional brain change analysis. Neuroimage 2002;17:479-489.

33. Smith SM, Nichols TE. Threshold-free cluster enhancement: addressing problems of smoothing, threshold dependence and localisation in cluster inference. Neuroimage 2009;44:83-98.

34. Winkler AM, Ridgway GR, Webster MA, Smith SM, Nichols TE. Permutation inference for the general linear model. Neuroimage 2014;92:381-397.

35. Schiff ND. Recovery of consciousness after brain injury: a mesocircuit hypothesis.

Trends Neurosci 2010;33:1-9.

36. Adams JH, Graham DI, Jennett B. The neuropathology of the vegetative state after an acute brain insult. Brain 2000;123 (Pt 7):1327-1338.

37. Fernandez-Espejo D, Junque C, Bernabeu M, Roig-Rovira T, Vendrell P, Mercader JM. Reductions of thalamic volume and regional shape changes in the vegetative and the minimally conscious states. J Neurotrauma 2010;27:1187-1193.

38. Lutkenhoff ES, McArthur DL, Hua X, Thompson PM, Vespa PM, Monti MM. Thalamic atrophy in antero-medial and dorsal nuclei correlates with six-month outcome after severe brain injury. Neuroimage Clin 2013;3:396-404.

39. Rosanova M, Gosseries O, Casarotto S, et al. Recovery of cortical effective connectivity and recovery of consciousness in vegetative patients. Brain 2012;135:1308-1320.

40. Varotto G, Fazio P, Rossi Sebastiano D, et al. Altered resting state effective connectivity in long-standing vegetative state patients: an EEG study. Clin Neurophysiol 2014;125:63-68.

41. Giacino JT, Whyte J, Bagiella E, et al. Placebo-controlled trial of amantadine for severe traumatic brain injury. N Engl J Med 2012;366:819-826.

42. Monti MM, Schnakers C, Korb AS, Bystritsky A, Vespa PM. Non-Invasive Ultrasonic Thalamic Stimulation in Disorders of Consciousness after Severe Brain Injury: A First-in-Man Report. Brain Stimul 2016;9:940-941.

43. Schiff ND, Giacino JT, Kalmar K, et al. Behavioural improvements with thalamic stimulation after severe traumatic brain injury. Nature 2007;448:600-603.

44. Schnakers C, Monti MM. Disorders of consciousness after severe brain injury: therapeutic options. Curr Opin Neurol 2017;30:573-579.

45. Thibaut A, Bruno MA, Ledoux D, Demertzi A, Laureys S. tDCS in patients with disorders of consciousness: sham-controlled randomized double-blind study. Neurology 2014;82:1112-1118.

46. Monti MM, Owen AM. Behavior in the Brain Using Functional Neuroimaging to Assess Residual Cognition and Awareness After Severe Brain Injury. Journal of Psychophysiology 2010;24:76-82.

47. Schnakers C, Giacino J, Kalmar K, Piret S, Lopez E. Does the FOUR Score Correctly Diagnose the Vegetative and Minimally Conscious States ? Tomographic Visualization of Cholinesterase. Ann Neurol 2006;60:2005-2006.

48. Schnakers C, Vanhaudenhuyse A, Giacino J, et al. Diagnostic accuracy of the vegetative and minimally conscious state: clinical consensus versus standardized neurobehavioral assessment. BMC Neurol 2009;9:35.

49. Edlow BL, Chatelle C, Spencer CA, et al. Early detection of consciousness in patients with acute severe traumatic brain injury. Brain 2017;140:2399-2414.

50. Masel BE, DeWitt DS. Traumatic Brain Injury: A Disease Process, Not an Event. Journal of Neurotrauma 2010;27:1529-1540.